Optical absorption and luminescence properties of Nd^{3+} in mixed alkali borate glasses—Spectroscopic investigations

Y.C. Ratnakaram[a,*], A. Vijaya kumar[a], D. Thirupathi Naidu[a], R.P.S. Chakradhar[b], K.P. Ramesh[b]

[a] *Department of Physics, S.V. University P.G. Centre, Kavali 524 201, Andhra Pradesh, India*
[b] *Indian Institute of Science, Bangalore 560012, India*

Abstract

Spectroscopic investigations were performed on $67B_2O_3 \cdot xLi_2O \cdot (32\text{-}x)Na_2O$ and $67B_2O_3 \cdot xLi_2O \cdot (32\text{-}x)K_2O$ (where $x = 8$, 12, 16, 20 and 24) glasses containing 1 mol% Nd_2O_3. Covalency was studied as a function of x using Judd-Ofelt intensity parameters that are related to the ligand field symmetry and the degree of bond covalency. Results show that covalency increases when the third component is added to the binary borate glass matrix. Various spectroscopic parameters like Racah (E^1, E^2 and E^3), spin–orbit (ξ_{4f}) and configuration interaction (α) parameters have been calculated. Using Judd-Ofelt intensity parameters (Ω_2, Ω_4 and Ω_6), total radiative transition probabilities (A_T), radiative lifetimes (τ_R), branching ratios (β) and integrated absorption cross sections ($\sum$) have been computed for certain excited states of Nd^{3+} in these mixed alkali borate glasses. From the luminescence spectra, effective line widths ($\Delta\lambda_{eff}$) and stimulated emission cross-sections (σ_p) have been reported for the three transitions $^4F_{3/2} \rightarrow {}^4I_{9/2}$, $^4F_{3/2} \rightarrow {}^4I_{11/2}$ and $^4F_{3/2} \rightarrow {}^4I_{13/2}$ of Nd^{3+}. Among all the glasses studied, lithium sodium glass with $x = 12$ and lithium potassium glass with $x = 20$ show high absorption and emission cross-sections.

Keywords: Absorption; Fluorescence; Radiative lifetime; Emission cross section

1. Introduction

Solid-state lasers have been employed in a vide variety of industrial and other applications. Rare earth elements in glasses have been widely studied for optical telecommunications and laser technology [1–6]. From the optical absorption measurements, the effect of host matrix on the local environments of a given rare earth cation with its first nearest neighbor anions such as oxygen can be elucidated using Judd-Ofelt [7,8] theory by studying changes of the experimentally fitted Judd–Ofelt intensity parameters, Ω_λ ($\lambda = 2$, 4 and 6). Gatterer et al. [9] studied Nd^{3+} in sodium borate and found that Ω_2 and Ω_4 were affected by the symmetry of

*Corresponding author. Tel.: +91-8626-43858; fax: +91-8626-41847.
E-mail address: ratnakaram_yc@yahoo.co.in (Y.C. Ratnakaram).

the crystal field around Nd^{3+} ions and bond covalency. Saisudha and Ramakrishna [10] studied the effect of PbO concentration on the Judd–Ofelt parameters of Nd^{3+}, Sm^{3+} and Dy^{3+} in borate glasses and showed that all the three parameters varied differently with PbO concentration. Binnemans et al. [11] gave optical properties of Nd^{3+} doped fluorophosphate glasses. Li et al. [12] reported the spectroscopy of neodymium (III) in alumino-borosilicate glasses. Recently, Kumar et al. [13] reported the stimulated emission and radiative properties of Nd^{3+} ions in barium fluorophosphates glass containing sulfate. De La Rosa-cruz et al. [14] reported the spectroscopic characterization of Nd^{3+} ions in barium fluorophosphate glasses.

For alkali borate glasses, the abrupt property changes were observed between 15 and 20 mol% modifier oxide [15]. This peculiar and anomalous behavior referred to as 'borate anomaly' was first explained in terms of the unique ability of boron to exist in two distinct co-ordination states–the trigonal and tetrahedral states. The addition of alkali oxide to boric oxide results in the conversion of boron from trigonal to tetrahedral co-ordination and at 20 mol% of R_2O (R = Li, Na, K and Rb) the tetraborate reaches maximum concentration, the boroxyl group disappears and the formation of diborate starts. Chong et al. [16] showed that mixed alkali borate glasses have structures that are quite similar to the binary borate glasses. In the recent past, we have studied the spectroscopic investigations of Nd^{3+} in $(Na_2O)_x(K_2O)_{30-x}(B_2O_3)_{70}$ ($x = 5$, 10, 15, 20 and 25) glasses and also influence of Nd^{3+} concentration on its optical absorption and luminescence properties in potassium borate glass [17,18].

In the present work, we report the spectroscopic and laser properties of Nd^{3+} doped borate glasses of the type $67B_2O_3 \cdot xLi_2O \cdot (32\text{-}x)Na_2O$ and $67B_2O_3 \cdot xLi_2O \cdot (32\text{-}x)K_2O$ (where $x = 8$, 12, 16, 20 and 24). The Judd-Ofelt theory has been applied to interpret the local environment of Nd^{3+} ion and bond covalency of Nd–O bond. Our main interest in the present study is to examine the variation of Judd–Ofelt intensity parameters, peak-to-peak intensity ratios, radiative lifetimes, the shape of the spectral profiles of the hypersensitive transition, emission peaks and emission cross sections with x in the above two glass matrices.

2. Experimental

Mixed alkali borate glasses containing Nd^{3+} ions were prepared using a regular melting technique. The details of preparation of these glasses were given in the authors earlier article [17]. The samples examined in the present work are $67B_2O_3 \cdot xLi_2O \cdot (32\text{-}x)Na_2O$ and $67B_2O_3 \cdot xLi_2O.(32\text{-}x)\ K_2O$ glasses with $x = 8$, 12, 16, 20 and 24 mol % . The glass compositions are the formal glass composition, although for the calculation of the various parameters, the actual composition was taken into account. The actual composition was calculated from the exact masses of the components in glass batch. There appears to be negligible weight loss during melting (± 0.005 g in a 5 g batch).

Optical absorption spectra of the polished samples in the visible range were recorded at room temperature using U3400 spectrophotometer. Luminescence spectra were also obtained at room temperature using Midac-FT photoluminescence spectrophotometer under excitation wavelength 514 nm of Ar^{3+} laser. The refractive indices of the samples were determined with an Abbe refractometer using monobromonaphthalene as an adhesive coating with an accuracy of ± 0.001 and the density measurements were made using Archemede's principle with xylene as immersion liquid to ± 0.02 g/cm^3. The sample thicknesses were obtained using a micrometer to ± 0.002 cm.

3. Results and analysis

3.1. Spectroscopic parameters

The room temperature optical absorption spectra of Nd^{3+} doped lithium sodium mixed alkali borate glasses in the wavelength range 300–1000 nm are shown in Fig. 1 for different x values in the glass matrix. The spectra of Nd^{3+} in the other glass matrix have not shown as it is similar in

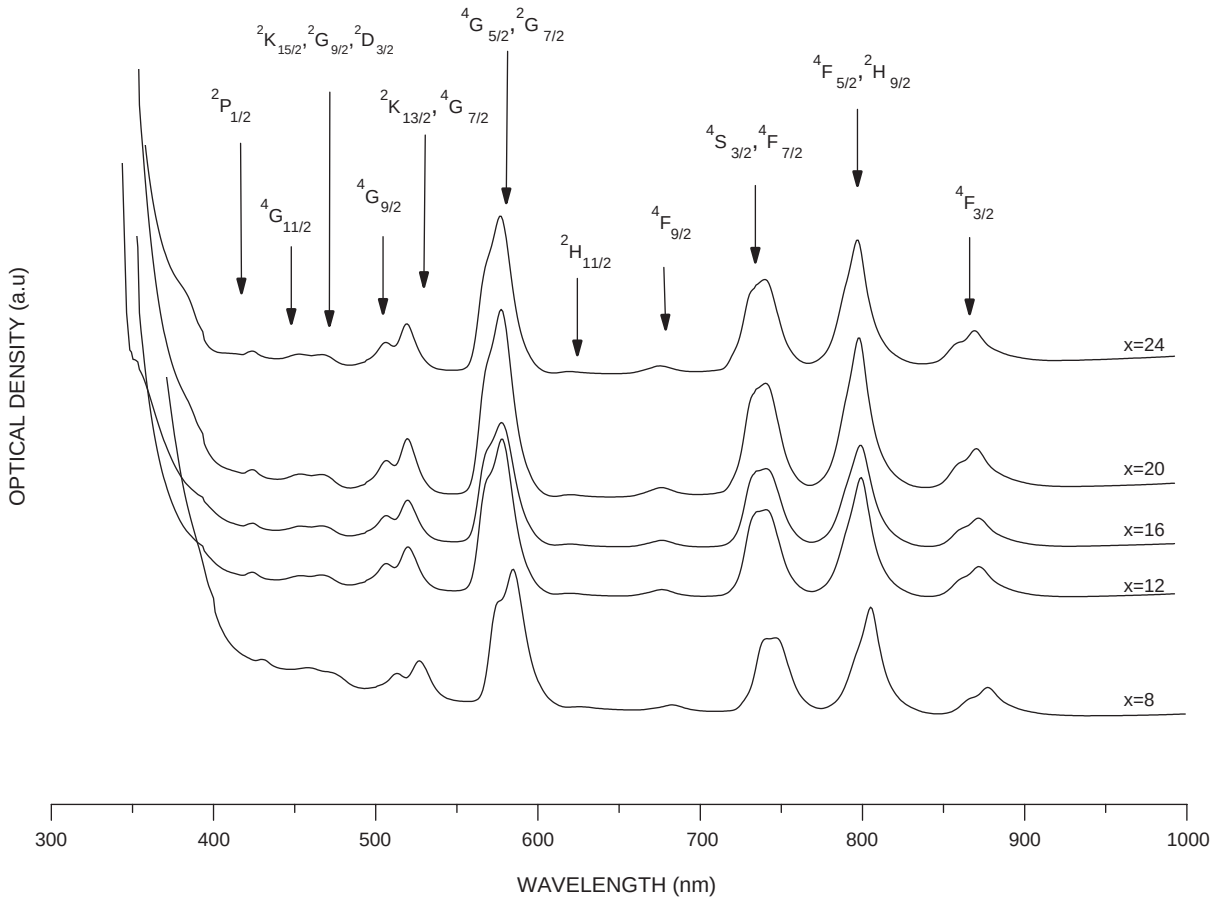

Fig. 1. Optical absorption spectra of Nd^{3+} doped $67B_2O_3.xLi_2O$. (32-x)Na_2O ($x=8$, 12, 16, 20 and 24) glasses

shape. The experimental energies of the observed levels of Nd^{3+} ion are presented in Table 1. The rms deviations between the experimental and calculated energies (using the method explained in Ref. [19]) are also presented in Table 1 and these values are very small which indicate that a full matrix diagonalization procedure leads to a good fit between the observed and calculated energies. The Racah (E^1, E^2, E^3), spin-orbit (ξ_{4f}) and configuration interaction (α) parameters obtained for all the glasses studied are presented in Table 1. The radial properties of Nd^{3+} are more or less same for all the mixed alkali borate glasses as indicated by the hydrogenic ratios (E^1/E^3 and E^2/E^3).

3.2. Spectral intensities and intensity parameters

The experimental (f_{exp}) spectral intensities of the absorption bands of rare earth ions are obtained from the relation [20]

$$f_{exp} = 4.318 \times 10^{-9} \int \epsilon(v)\,dv, \quad (1)$$

where $\epsilon(v)$ is the molar absorption co-efficient in $(\text{mol cm})^{-1}$ and v is the transition energy in cm^{-1}. The main contributions to the intensity of a transition between two electronic states of a rare earth ion are the electric dipole and magnetic dipole contributions. The f–f transitions are predominantly electric dipole in nature. The

Table 1
Experimental energies (E_{exp}) and various spectroscopic parameters (E^1, E^2, E^3, ξ_{4f} and α) of Nd^{3+} doped $67B_2O_3 \cdot xLi_2O \cdot (32\text{-}x)Na_2O$ (LSG) and $67B_2O_3 \cdot xLi_2O \cdot (32\text{-}x)\ K_2O$ (LPG) glasses

S. no	Energy level	LSG					LPG				
		$x = 8$	$x = 12$	$x = 16$	$x = 20$	$x = 24$	$x = 8$	$x = 12$	$x = 16$	$x = 20$	$x = 24$
1	$^4F_{3/2}$	11399	11386	11386	11399	11412	11361	11386	11373	11412	11373
2	$^4F_{5/2}$, $^2H_{9/2}$	12418	12403	12403	12434	12434	12373	12403	12403	12434	12403
3	$^4F_{7/2}$, $^4S_{3/2}$	13401	13383	13383	13383	13383	13492	13509	13491	13401	13365
4	$^4F_{9/2}$	14573	14616	14637	14637	14658	14616	14689	14615	14659	14616
5	$^2H_{11/2}$	15975	15975	15975	16018	15970	15970	15995	15944	15970	15945
6	$^4G_{5/2}$, $^2G_{7/2}$	17118	17118	17118	17118	17118	17089	17089	17089	17089	17089
7	$^2K_{13/2}$, $^4G_{7/2}$	18970	19006	19006	19006	19006	18863	18934	18970	18970	19006
8	$^4G_{9/2}$	19488	19487	19487	19487	19487	19488	19526	19488	19487	19488
9	$^2K_{15/2}$, $^2G_{9/2}$,$^2D_{3/2}$	21230	21158	21086	21082	20998	—	21180	21091	21047	21047
10	$^4G_{11/2}$	21780	21752	21828	21827	21733	—	21780	21780	21780	21780
11	$^2P_{1/2}$	23249	23195	23249	23195	23249	23249	23195	23249	23195	23249
	rms deviation	±120	±87	±94	±97	±79	±92	±99	±109	±89	±91
	E^1	5110	5110	5117	5088	5101	5075	5046	5088	5073	5127
	E^2	27.1	26.5	27.5	27.2	26.5	21.8	26.3	26.9	26.8	27.1
	E^3	492.2	493.0	493.4	493.0	491.6	483.4	488.5	490.2	491.2	493.6
	ξ_{4f}	921.8	916.5	931.6	930.5	915.2	834.5	934.8	928.9	925.4	922.2
	α	7.56	7.83	9.31	8.39	5.96	6.32	4.32	6.14	6.27	9.12
	E^1/E^3	10.38	10.36	10.37	10.32	10.37	10.49	10.34	10.37	10.32	10.38
	E^2/E^3	0.055	0.053	0.055	0.055	0.054	0.045	0.054	0.055	0.054	0.055

magnetic dipolar contributions are negligible. The theoretical oscillator strengths, f_{cal} of the electric dipole transitions, within the f^N configurations can be calculated using Judd–Ofelt [7,8] theory, in terms of three intensity parameters Ω_2, Ω_4 and Ω_6 using the relation

$$f_{cal}(aJ, bJ') = \frac{8\prod^2 mcv\ (n^2+2)^2}{3h(2J+1)\quad 9n} \times \sum_{\lambda=2,4,6} \Omega_\lambda |<(SLJ)||U^\lambda||(S'L'J')>|^2, \qquad (2)$$

where $\|U^\lambda\|^2$ represents the square of the reduced matrix elements of the unit tensor operator U^λ connecting the initial and final states. Because of the electrostatic shielding of the 4f electrons by the closed 5p shell electrons, the matrix elements of the unit tensor operator between two energy manifolds in a given rare-earth ion do not vary significantly when it is incorporated in different hosts. Hence, we have taken the values of doubly reduced matrix elements of unit tensor operator given by Carnall et al. [21]. Substituting the 'f_{meas}' for 'f_{cal}' and using the squared reduced matrix elements the three intensity parameters, Ω_2, Ω_4 and Ω_6 are obtained. Generally Ω_2 parameter is an indicator of covalency of metal ligand bond and Ω_4 and Ω_6 parameters are related to the rigidity of the host matrix. The intensities of most of the transitions are low in glasses with $x = 20$ in lithium sodium glass and with $x = 8$ in lithium potassium glass. It indicates that the crystal field asymmetry at the site of Nd^{3+} is low at $x = 20$ in lithium sodium glass and at $x = 8$ in lithium potassium glass.

The best set of Judd–Ofelt intensity parameters (Ω_2, Ω_4 and Ω_6) obtained from a least square analysis of the observed oscillator strengths for all the mixed alkali borate glasses are presented in Table 2. The Judd–Ofelt parameters in binary sodium borate, potassium borate and lithium borate glasses are also presented in the table. From the table it is observed that Ω_2 parameter increases, compared to their values in binary

Table 2
Judd–Ofelt intensity parameters ($\Omega_\lambda \times 10^{20}$) ($cm^2$) and peak intensity ratios (I_L/I_S) of hypersensitive transition of Nd^{3+} doped mixed alkali borate glasses

S. no	Glass matrix	Ω_2	Ω_4	Ω_6	$\Sigma\Omega_\lambda$	I_L/I_S	Ref.
1	$8Li_2O + 24Na_2O + 67B_2O_3$	8.81 ± 0.78	6.78 ± 0.68	9.01 ± 0.88	24.60 ± 2.42	—	Present work
2	$12Li_2O + 20Na_2O + 67B_2O_3$	9.59 ± 0.92	7.87 ± 0.72	9.84 ± 0.98	27.32 ± 2.63	—	Present work
3	$16Li_2O + 16Na_2O + 67B_2O_3$	8.39 ± 0.75	6.51 ± 0.61	10.01 ± 1.04	24.92 ± 2.32	—	Present work
4	$20Li_2O + 12Na_2O + 67B_2O_3$	7.57 ± 0.69	7.01 ± 0.67	8.86 ± 0.82	23.45 ± 2.13	—	Present work
5	$24Li_2O + 8Na_2O + 67B_2O_3$	8.53 ± 0.82	7.47 ± 0.70	9.60 ± 0.87	25.61 ± 2.22	—	Present work
6	$8Li_2O + 24K_2O + 67B_2O_3$	7.94 ± 0.77	3.57 ± 0.28	7.94 ± 0.78	19.45 ± 1.66	1.032	Present work
7	$12Li_2O + 20K_2O + 67B_2O_3$	10.83 ± 0.93	7.73 ± 0.74	9.04 ± 0.86	27.61 ± 2.52	1.091	Present work
8	$16Li_2O + 16K_2O + 67B_2O_3$	10.28 ± 0.89	8.12 ± 0.78	10.58 ± 0.96	28.98 ± 2.64	1.113	Present work
9	$20Li_2O + 12K_2O + 67B_2O_3$	11.08 ± 1.03	8.92 ± 0.84	11.57 ± 1.05	31.49 ± 2.87	1.123	Present work
10	$24Li_2O + 8K_2O + 67B_2O_3$	11.52 ± 1.06	9.55 ± 0.91	13.62 ± 1.25	34.69 ± 3.32	1.230	Present work
11	$5Na_2O + 25K_2O + 70B_2O_3$	8.11 ± 0.78	5.25 ± 0.48	4.96 ± 0.47	18.32 ± 1.72	0.947	[17]
12	$10Na_2O + 20K_2O + 70B_2O_3$	11.06 ± 1.10	7.97 ± 0.81	7.79 ± 0.76	26.82 ± 2.40	1.000	[17]
13	$15Na_2O + 15K_2O + 70B_2O_3$	10.72 ± 0.93	7.31 ± 0.72	7.47 ± 0.73	25.50 ± 2.12	1.085	[17]
14	$20Na_2O + 10K_2O + 70B_2O_3$	14.29 ± 1.32	8.83 ± 0.77	9.76 ± 0.93	32.88 ± 3.14	1.107	[17]
15	$25Na_2O + 5K_2O + 70B_2O_3$	13.30 ± 1.25	9.07 ± 0.88	10.09 ± 0.98	32.46 ± 3.13	1.111	[17]
16	$30Na_2O + 70B_2O$	4.91	3.28	4.51	12.70	—	[27]
17	$30K_2O + 70B_2O$	4.94	3.10	3.42	11.46	—	[27]
18	$30Li_2O + 70B_2O$	4.20	3.89	4.74	12.83	—	[27]

sodium borate or potassium borate or lithium borate glasses, when the third component is added to the glass matrix. It indicates that the covalency increases when the third component is added to the glass matrix. In the present work, Ω_2 parameter is high at $x = 12$ and low at $x = 20$ in the case of lithium sodium glass, whereas in lithium potassium glass it is high at $x = 24$ and low at $x = 8$. It suggests strong covalency at $x = 12$ and 24 in lithium sodium and lithium potassium glasses, respectively. Though the Ω_2 parameter is an indicator for covalent bonding, in view of hypersensitivity, Oomen and Van Dongen [22] suggested that instead of observing the variation in Ω_2 alone, it is appropriate to see the variation of the sum of the Judd–Ofelt parameters $\Sigma\Omega_\lambda$, which also increase with increasing covalency. $\Sigma\Omega_\lambda$ values for all the mixed alkali borate glasses and also for binary borate glasses are also presented in Table 2. From the table it is observed that $\Sigma\Omega_\lambda$ value is high at $x = 12$ and low at $x = 20$ for lithium sodium glass and $\Sigma\Omega_\lambda$ is high at $x = 24$ and low at $x = 8$ for lithium potassium glass. Hence, $\Sigma\Omega_\lambda$ values also suggest similar covalency (high at $x = 12$ for lithium sodium glass and at $x = 24$ for lithium potassium glass). Variation of Ω_2 parameter with x is shown in Fig. 2 for both lithium sodium (LSG) and lithium potassium (LPG) glasses. Ω_λ can also be written as

$$\Omega_\lambda = (2t+1)\sum_{s,p} |A_{s,p}|^2 \Xi^2(s,t)(2s+1)^{-1}, \quad t = 2,4,6, \tag{3}$$

where $A_{s,\,p}$ are the crystal field parameters of rank s and are related to the structure around rare earth ions. $\Xi(s,t)$ is related to the matrix elements between the two radial wave functions of 4f and the admixing levels e.g., 5d, 5g and the energy difference between these levels. It has been suggested by Reisfeld [23] that Ξ correlates to the nephelauxetic parameter β, which indicates the degree of covalency of the R–O bond.

3.3. Hypersensitive transition

For Nd^{3+} ion, $^4I_{9/2} \rightarrow {}^4G_{5/2} + {}^2G_{7/2}$ is the hypersensitive transition. It follows the selection rules $\Delta J \leqslant 2$, $\Delta L \leqslant 2$, and $\Delta S = 0$. The position and intensity of the hypersensitive transition are found to be very sensitive to the environment of the rare earth ion. In the present work, it is

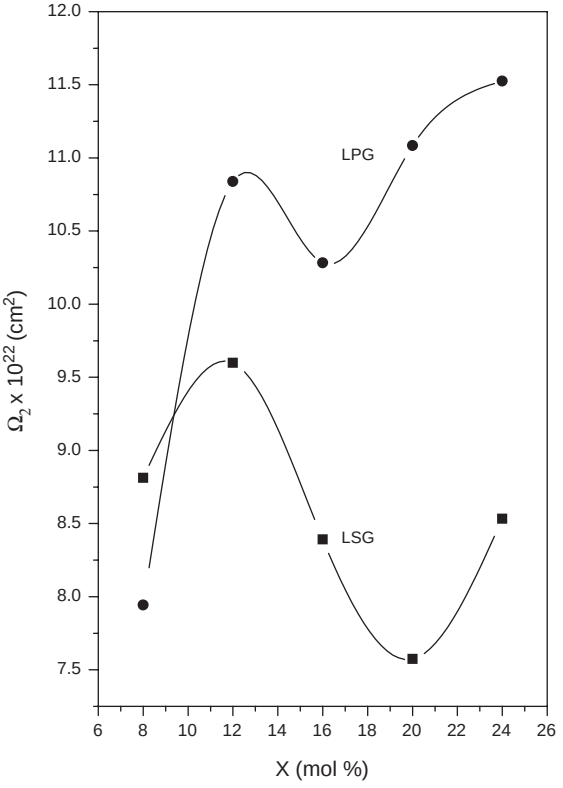

Fig. 2. Variation of Ω_2 (x 10^{20}) with x in lithium sodium (LSG) and lithium potassium (LPG) mixed alkali borate glasses.

observed that there is no change in the position of the peak wavelength of the hypersensitive transition with x in both the mixed alkali borate glasses. A careful investigation was carried out on the variation of the spectral profile of the hypersensitive transition with glass composition to monitor the covalency of the Nd–O bond in the glass matrix based on nephelauxetic effect.

The hypersensitive transition in the absorption spectra of Nd^{3+} doped glasses is split into two peaks by the Stark splitting due to crystal field. It was observed that whenever the glass composition varied the relative intensity ratio between the peaks also varied. The peak intensity ratios of the longer and smaller wavelength components are designated as I_L/I_S. An increase in the intensity ratio I_L/I_S is found indicating a shift of the center of gravity of the absorption spectra to longer wavelength [24] which indicates an increase in covalency of Nd-O bond. The present investigation reveals that the Stark splitting of the transition $^4I_{9/2} \rightarrow {}^4G_{5/2} + {}^2G_{7/2}$ is not resolved in lithium sodium glass. In the case of lithium potassium glass, there is clear splitting for $x = 8$, 12 and 16. For $x = 20$ and 24 mol% the splitting is decreased and the relative intensities of the components changed, so that the splitting is hidden by the inhomogeneous broadening. However, the intensity of the peak at longer wavelength increases. I_L/I_s values in this glass matrix are 1.032, 1.091, 1.113, 1.123 and 1.23 for $x = 8$, 12, 16, 20 and 24, which indicate that the covalency of Nd–O bond is increasing with the increase of lithium content in lithium potassium glass. Variation of spectral profile of the hypersensitive transition with x is shown in Fig. 3 for both lithium sodium (LSG) and lithium potassium (LPG) glasses.

The analysis of the present work reveals that as there is no shift in peak wavelength of the hypersensitive transition and also as there is no peak splitting of the hypersensitive transition in lithium sodium glass, it is observed from Eq. (3) that $|A_{s,P}|$ alone is responsible for the decrease or increase of Ω_2. The decrease in Ω_2 parameter from 9.59×10^{-20} to 7.57×10^{-20} cm^2 with the increase of x from 12% to 20 mol% indicating the structural changes (conversion of boron from trigonal to tetrahedral coordination) at these compositions. In lithium potassium glass, even though there is no change in the peak wavelength of hypersensitive transition, the peak intensity ratios are increasing with the increase of lithium content (x), which indicates increasing covalency. In this glass, except at $x = 16$ mol%, Ω_2 parameter increases with the increase of x in the glass matrix. From Eq. (3), it is observed that $|A_{s,P}|$ alone is responsible for the decrease of Ω_2 parameter at $x = 16$ mol%. It indicates structural changes at this composition. From Table 4, it is also observed that the covalency decreases at $x = 16$ mol% (i.e., at equal mole percentages) for all the three mixed alkali borate glasses.

3.4. Radiative properties

The Ω_λ values thus obtained from the absorption measurements are used to calculate the

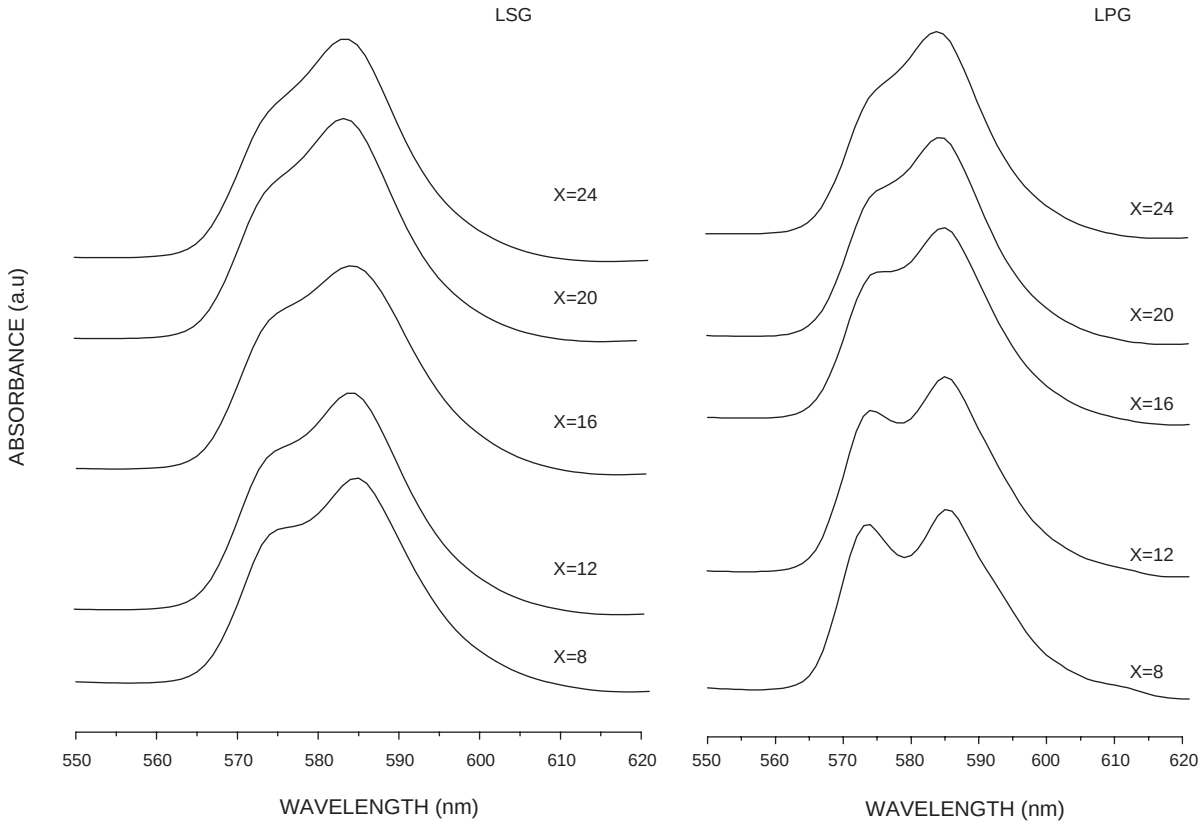

Fig. 3. Variation of spectral profiles of hypersensitive transition $^4F_{3/2} \rightarrow {}^4G_{5/2} + {}^2G_{7/2}$ with x in lithium sodium (LSG) and lithium potassium (LPG) mixed alkali borate glasses.

radiative transition probabilities, radiative lifetimes and branching ratios using the theory explained in Ref. [25]. Estimated total radiative transition probabilities (A_T) and radiative lifetimes (τ_R) for the excited states $^4G_{9/2}$, $^4G_{7/2}$, $^4G_{5/2}$, $^2H_{11/2}$, $^4F_{9/2}$, $^4F_{5/2}$ and $^4F_{3/2}$ of Nd^{3+} in different mixed alkali borate glasses are presented in Table 3. It is observed from the table that the total spontaneous transition probabilities of all the excited states of Nd^{3+} increases with increasing covalency of the rare earth site (Ω_2 value). Takebe et al. [24] reported similar results in other oxide glasses. Variation of A_T with x is shown in Fig. 4 for both lithium sodium and lithium potassium glasses. The radiative lifetime represents an effective average over site-site variations in the local Nd^{3+} environment. The error in the estimated radiative lifetimes is nearly $\pm 10\%$ for all the excited states. It is observed that the estimated radiative lifetimes of the excited states are low at $x = 12$ and high at $x = 20$ in lithium sodium glass. In lithium potassium glass, the lifetimes of all the states are high at $x = 8$ and low at $x = 24$ and these values are decreasing with the increase of x. The branching ratios (β) and integrated absorption cross-sections (Σ) for certain transitions of Nd^{3+}, which have higher magnitudes are presented in Table 4 for both lithium sodium and lithium potassium glasses. From the table it is observed that integrated absorption cross-sections are high at $x = 12$ and low at $x = 20$ in lithium sodium glass, whereas in lithium potassium glass, Σ values are high at $x = 24$ and low at $x = 8$. The branching ratios are highest for $^4G_{5/2} \rightarrow {}^4I_{9/2}$ transition in the both glasses. From the magnitude of integrated absorption cross-sections, it is

Table 3
Total radiative transition probabilities (A_T) (s^{-1}) and radiative lifetimes (τ_R)(μs) of certain excited states of Nd^{3+} doped $67B_2O_3 \cdot xLi_2O \cdot (32\text{-}x)Na_2O$ (LSG) and $67B_2O_3 \cdot xLi_2O \cdot (32\text{-}x)\ K_2O$ (LPG) glasses

S. no	Glass	$^4G_{9/2}$		$^4G_{7/2}$		$^4G_{5/2}$		$^2H_{11/2}$		$^4F_{9/2}$		$^4F_{5/2}$		$^4F_{3/2}$	
		A_T	τ_R	A_T	τ_R	A_T	τ_R	A_T	τ_R	A_T	τ_R	A_T	τ_R	A_T	τ_R
	LSG														
1	$x = 8$	23121	43	21794	45	33521	29	917	1090	6142	162	7239	136	5494	181
2	$x = 12$	26117	38	24428	40	37536	26	987	1013	6859	145	8119	123	6195	161
3	$x = 16$	22720	44	21405	46	32773	30	944	1058	6624	150	7691	130	5751	173
4	$x = 20$	21701	46	20263	49	31136	32	861	1161	6085	164	7254	138	5496	182
5	$x = 24$	24291	41	22344	44	34207	29	927	1079	6738	148	7951	125	6066	164
	LPG														
6	$x = 8$	19052	52	17372	57	25713	38	545	1834	5376	185	5769	173	4461	224
7	$x = 12$	26936	37	25526	39	39259	25	975	1025	6382	156	7656	130	5807	172
8	$x = 16$	27305	36	25674	38	39398	25	1062	941	7280	137	8609	116	6515	153
9	$x = 20$	29685	33	27906	35	42922	23	1138	878	7964	125	9449	105	7163	139
10	$x = 24$	31877	31	29798	33	45599	21	1287	777	9127	109	10639	93	8033	124

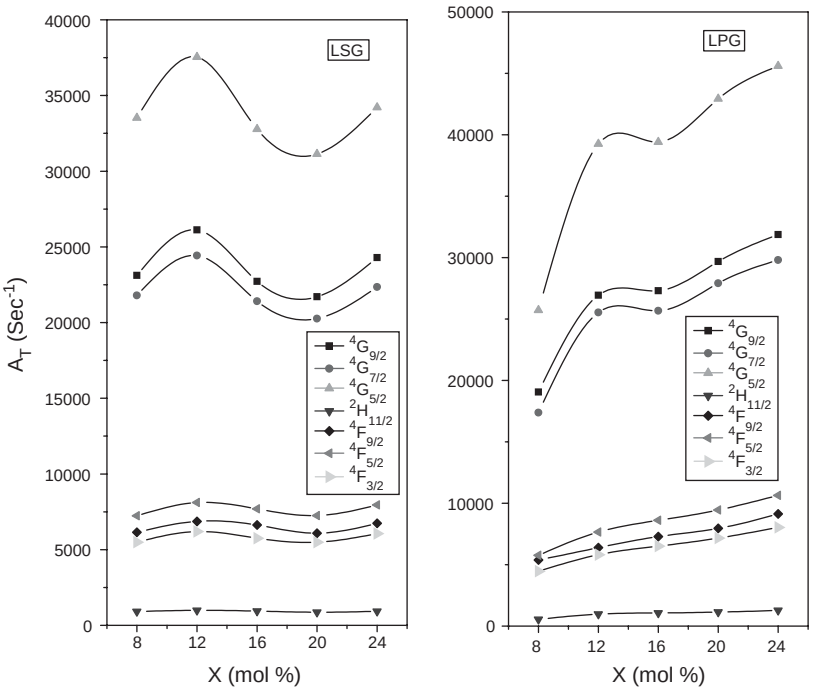

Fig. 4. Variation of total radiative transition probabilities (A_T) with x in lithium sodium (LSG) and lithium potassium (LPG) mixed alkali borate glasses.

observed that among all the glasses studied, lithium sodium glass with $x = 12$ and lithium potassium glass with $x = 24$ are favorable for laser excitation.

3.5. Fluorescence spectra

Good laser transitions are characterized by large cross-sections for stimulated emission. The

Table 4
Branching ratios (β) and integrated absorption cross sections ($\sum \times 10^{18}\,cm^{-1}$) of certain transitions of Nd^{3+} doped $67B_2O_3 \cdot xLi_2O \cdot (32\text{-}x)Na_2O$ (LSG) and $67B_2O_3 \cdot xLi_2O \cdot (32\text{-}x)\,K_2O$ (LPG) glasses

S. no.	Glass	$^4G_{9/2} \rightarrow {}^4I_{13/2}$		$^4G_{7/2} \rightarrow {}^4I_{11/2}$		$^4G_{5/2} \rightarrow {}^4I_{9/2}$		$^4H_{11/2} \rightarrow {}^4I_{15/2}$		$^4F_{5/2} \rightarrow {}^4I_{9/2}$		$^4F_{3/2} \rightarrow {}^4I_{9/2}$		$^4F_{3/2} \rightarrow {}^4I_{11/2}$		$^4F_{3/2} \rightarrow {}^4I_{13/2}$	
		β	$\sum$	β	$\sum$	β	$\sum$	β	$\sum$	β	$\sum$	β	$\sum$	β	$\sum$	β	$\sum$
	LSG																
1	$x = 8$	0.152	24.6	0.558	20.5	0.811	45.2	0.514	2.0	0.664	15.3	0.395	8.3	0.505	15.5	0.096	4.9
2	$x = 12$	0.508	27.3	0.551	22.5	0.807	50.2	0.518	2.5	0.661	17.1	0.402	9.5	0.499	17.2	0.094	5.4
3	$x = 16$	0.449	23.5	0.546	19.6	0.804	43.5	0.486	1.9	0.671	16.3	0.377	8.2	0.518	16.7	0.098	5.4
4	$x = 20$	0.491	22.1	0.529	18.0	0.797	41.1	0.491	1.8	0.666	15.3	0.404	8.5	0.499	15.4	0.093	4.8
5	$x = 24$	0.498	24.8	0.538	20.1	0.801	45.2	0.507	2.0	0.661	16.6	0.397	9.1	0.502	16.8	0.097	5.3
	LPG																
6	$x = 8$	0.553	20.6	0.620	17.8	0.833	36.1	0.579	1.5	0.642	11.8	0.306	5.1	0.557	13.0	0.091	4.6
7	$x = 12$	0.529	29.6	0.578	24.9	0.826	54.1	0.539	2.4	0.665	16.1	0.416	9.2	0.491	16.0	0.092	4.9
8	$x = 16$	0.509	28.8	0.555	24.0	0.811	53.1	0.511	2.3	0.666	18.1	0.399	9.9	0.502	18.3	0.094	5.7
9	$x = 20$	0.507	31.2	0.551	25.9	0.809	57.6	0.510	2.5	0.664	19.9	0.399	10.9	0.502	20.1	0.095	6.3
10	$x = 24$	0.497	32.8	0.541	27.1	0.801	60.6	0.494	2.7	0.666	22.6	0.385	11.8	0.512	23.1	0.099	7.4

Judd-Ofelt theory can successfully account for the induced emission cross-sections that are observed. The peak stimulated emission cross-section, σ_p is related to the radiative transition probability $A(aJ, bJ')$ by [25]

$$\sigma_p = \frac{\lambda_p^4}{8\Pi c n^2 \Delta\lambda_{\text{eff}}} A_{\text{rad}}(aJ, bJ'), \tag{4}$$

where λ_p is the peak wavelength and $\Delta\lambda_{\text{eff}}$ is the effective line width of the emission band. From the above Eq. (4) σ_p depends on the intensity parameters Ω_λ, the bandwidth $\Delta\lambda_{\text{eff}}$ and the refractive index n. Both Ω_λ and $\Delta\lambda_{\text{eff}}$ are affected by compositional changes. The luminescence spectra of Nd^{3+} in lithium sodium mixed alkali borate glasses recorded at room temperature in the region 6000–12000 cm^{-1}, under excitation wavelength 514 nm of Ar^{3+} laser are shown in Fig. 5. The emission spectra in the other glass matrix have not shown, as it is similar in shape. In the emission spectra, three bands, a broad band at $\cong$880 nm, a strong band at $\cong$1060 nm and another band at $\cong$1330 nm are identified. These bands are assigned to the transitions $^4F_{3/2} \rightarrow {}^4I_{9/2}$, $^4F_{3/2} \rightarrow {}^4I_{11/2}$ and $^4F_{3/2} \rightarrow {}^4I_{13/2}$ respectively. In the observed luminescence spectra, $^4F_{3/2} \rightarrow {}^4I_{11/2}$ transition consists of overlapping lines arising from transitions between the split $^4F_{3/2}$ level and various sublevels of $^4I_{11/2}$ states. The sharp peak at $\cong$1060 nm i.e. $^4F_{3/2} \rightarrow {}^4I_{11/2}$ transition composed of two peaks and the separation between the peaks varies with x. The peak-to-peak separation is 244, 236, 227, 240 and 240 cm^{-1} for $x = 8$, 12, 16, 20 and 24 in lithium sodium glass matrix. In the case of lithium potassium glass, the peak-to-peak separation is 278, 267, 280, 244 and 240 cm^{-1} for $x = 8$, 12, 16, 20 and 24. It is observed from the shape of the spectral profile of $^4F_{3/2} \rightarrow {}^4I_{11/2}$ transition that as x increases from 8 to 16, the intensity of the small peak decreases and for $x = 20$, the intensity increases in lithium sodium glass. However, when $x = 24$, a marginal decline is observed when compared to $x = 20$. In the case of lithium potassium glass, as x increases from 8 to 24, the intensity of the small peak decreases. It indicates structural variations and the accompanying changes in the Nd-O bond, due to increase in lithium content in lithium sodium and lithium potassium glasses. Similar type of variations is observed in the spectral profile of the hypersensitive transition for lithium sodium and lithium potassium glasses.

Table 5 gives peak wavelengths (λ_P), radiative transition probabilities (A_{rad}), effective linewidths ($\Delta\lambda_{\text{eff}}$) and stimulated emission cross-sections (σ_p) of $^4F_{3/2} \rightarrow {}^4I_{13/2}$, $^4F_{3/2} \rightarrow {}^4I_{11/2}$ and $^4F_{3/2} \rightarrow {}^4I_{9/2}$

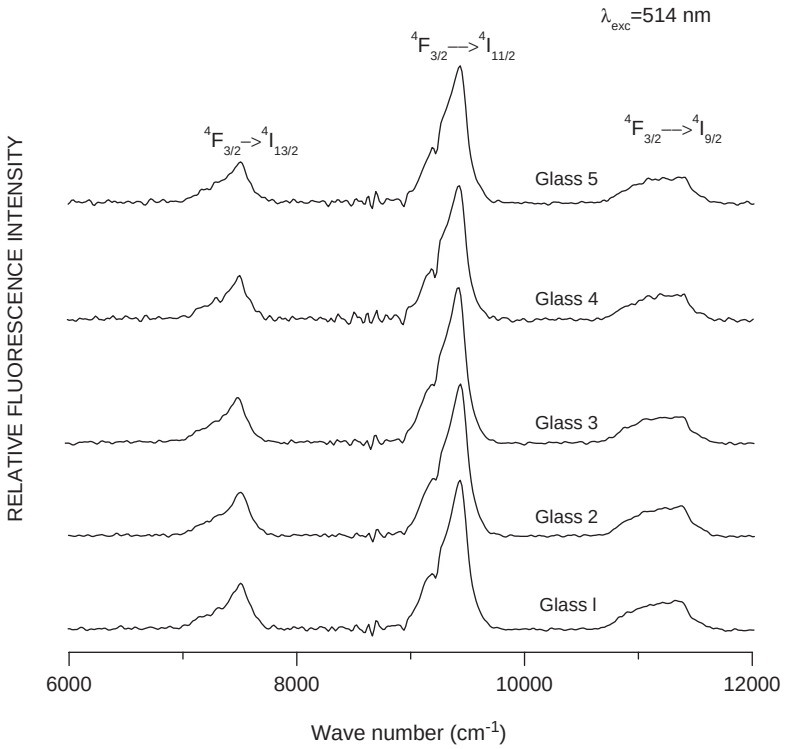

Fig. 5. Luminescence spectra of Nd^{3+} in $67B_2O_3.xLi_2O$. (32-x) Na_2O ($x = 8$, 12, 16, 20 and 24) glasses.

Table 5
Certain fluorescence properties of Nd^{3+} doped $67B_2O_3 \cdot xLi_2O \cdot (32\text{-}x)Na_2O$ (LSG) and $67B_2O_3 \cdot xLi_2O \cdot (32\text{-}x)\ K_2O$ (LPG) glasses

S. no	Glass	$^4F_{3/2} \rightarrow\ ^4I_{13/2}$				$^4F_{3/2} \rightarrow\ ^4I_{11/2}$				$^4F_{3/2} \rightarrow\ ^4I_{9/2}$			
		λ_P (nm)	A_{rad} (s^{-1})	$\Delta\upsilon$ $(cm)^{-1}$	σ_P ($10^{-20}\,cm^2$)	λ_P (nm)	A_{rad} (s^{-1})	$\Delta\upsilon$ $(cm)^{-1}$	σ_P ($10^{-20}\,cm^2$)	λ_P (nm)	A_{rad} (s^{-1})	$\Delta\upsilon$ $(cm)^{-1}$	σ_P ($10^{-20}\,cm^2$)
	LSG												
1	$x = 8$	1330	528	270	1.70	1060	2773	276	5.59	887	2169	551	1.52
2	$x = 12$	1340	585	321	1.61	1069	3092	280	6.16	902	2491	546	1.82
3	$x = 16$	1330	576	281	1.78	1050	2980	270	6.04	884	2170	608	1.36
4	$x = 20$	1330	511	253	1.76	1060	2742	283	5.38	884	2220	568	1.48
5	$x = 24$	1320	582	309	1.60	1058	3047	278	5.98	884	2410	561	1.64
	LPG												
6	$x = 8$	1330	577	327	1.54	1050	2486	327	4.20	883	1365	619	0.84
7	$x = 12$	1330	520	520	1.51	1050	2850	309	5.09	883	2414	570	1.62
8	$x = 16$	1330	615	615	2.14	1050	3272	246	7.34	881	2600	497	1.99
9	$x = 20$	1330	679	679	2.15	1050	3596	282	7.03	882	2857	534	2.04
10	$x = 24$	1330	792	792	2.48	1050	4110	257	8.84	893	3095	470	2.58

transitions. The emission band $^4F_{3/2} \rightarrow\ ^4I_{11/2}$ at $\cong$ 1060 nm has been considered as potential lasing transition due to the large stimulated emission cross-section. The large stimulated emission cross-sections are attractive features for low threshold, high gain applications and are utilized to obtain

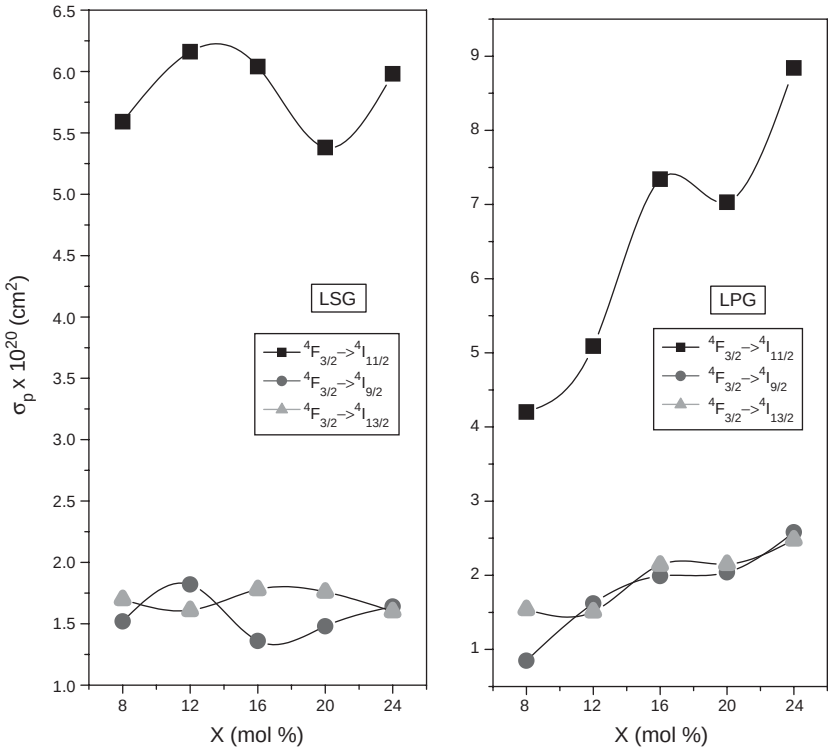

Fig. 6. Variation of emission cross-section (σ_P) with x in lithium sodium (LSG) and lithium potassium (LPG) mixed alkali borate glasses.

CW laser action. These values for $^4F_{3/2} \rightarrow {}^4I_{11/2}$ transition are high for lithium sodium and lithium potassium glasses when compared with sodium potassium glass [17]. It is also observed that σ_p value increases when the third component is added to the glass matrix [26]. Among all the glasses studied in the present work, lithium sodium glass with $x = 12$ and lithium potassium glass with $x = 24$ have higher stimulated emission cross-sections for the above transition. Variation of σ_p with x is shown in Fig. 6 for both lithium sodium (LSG) and lithium potassium (LPG) glasses. Certain fluorescence properties of $^4F_{3/2} \rightarrow {}^4I_{11/2}$ transition are compared with various other glass matrices in Table 6. It is observed from the table that emission cross sections are high in the mixed alkali borate glasses when compared with borate glass. The results of the present investigations conclude that lithium sodium glass with $x = 12$ and lithium potassium glass with $x = 24$ are more suitable for laser excitation.

4. Conclusions

The spectral intensities of most of the transitions are low in glasses with $x = 20$ in lithium sodium glass and with $x = 8$ in lithium potassium glass which indicate that the crystal field asymmetry is low at $x = 20$ in lithium sodium and at $x = 8$ in lithium potassium glass. Ω_2 parameter is high at $x = 12$ and low at $x = 20$ in the case of lithium sodium glass, whereas in lithium potassium glass this parameter is high at $x = 24$ and low at $x = 8$ thus suggesting strong covalency at $x = 12$ and at $x = 24$ in lithium sodium and lithium potassium glasses, respectively. The Judd-Ofelt intensity parameter Ω_2 is increased, when the third component is added to the glass matrix, which indicates increase in covalency with the addition of second alkali in the glass matrix. The hypersensitive transition $^4I_{9/2} \rightarrow {}^4G_{5/2} + {}^2G_{7/2}$ is not resolved into two peaks by Stark splitting in lithium sodium glass and also there is no shift in the peak

Table 6
Comparison of certain fluorescence properties of Nd^{3+} doped mixed alkali borate glasses with other glass matrices

S. no.	Glass	$^4F_{3/2} \rightarrow {}^4I_{11/2}$				Ref.
		λ_p (nm)	A_{rad} (s^{-1})	$\Delta\upsilon$ $(cm)^{-1}$	σ_P ($10^{-20}cm^2$)	
	LSG					
1	$x = 8$	1060	2773	276	5.59	Present work
2	$x = 12$	1069	3092	280	6.16	Present work
3	$x = 16$	1050	2980	270	6.04	Present work
4	$x = 20$	1060	2742	283	5.38	Present work
5	$x = 24$	1058	3047	278	5.98	Present work
	LPG					
6	$x = 8$	1050	2486	327	4.20	Present work
7	$x = 12$	1050	2850	309	5.09	Present work
8	$x = 16$	1050	3272	246	7.34	Present work
9	$x = 20$	1050	3596	282	7.03	Present work
10	$x = 24$	1050	4110	257	8.84	Present work
11	Borate	1054–1062	3700–2220	294-263	2.1–3.2	[28]
12	Phosphate	1052–1057	3570–1890	454-285	2.0–4.8	[28]
13	Tellurite	1056–1063	7140–4160	384-322	3.0–5.1	[28]
14	Sulfide	1075–1077	15620–10000	476	6.9–8.2	[28]
15	Chloride	1062–1064	5550–4540	526-500	6.0–6.3	[28]

wavelength of the transition in this glass matrix. Hence $A_{s,p}$ is alone responsible for the increase or decrease in Ω_2 parameter. In the case of lithium potassium glass, there is a clear splitting and the peak intensity ratios are increasing with the increase of lithium content indicating the increase in covalency of Nd-O bond.

The total spontaneous transition probabilities (A_T) of all the excited states of Nd^{3+} increased with the increase of covalency of the rare earth site. The estimated radiative lifetimes (τ_R) of all the excited states are low at $x = 12$ and high at $x = 20$ in lithium sodium glass. In lithium potassium glass, the lifetimes of all the states are high at $x = 8$ and low at $x = 24$. The branching ratios are highest for $^4G_{5/2} \rightarrow {}^4I_{9/2}$ transition in both the glasses. From the shape of the spectral profile of the emission band, $^4F_{3/2} \rightarrow {}^4I_{11/2}$, it is observed that as x increases from 8 to 16, the intensity of the small peak decreases and for $x = 20$, the intensity increases in lithium sodium glass. At $x = 24$, a marginal decline is observed. In the case of lithium potassium glass, as x increases from 8 to 24, the intensity of the small peak decreases. It indicates structural variations and the accompanying changes in the Nd-O bond. The stimulated emission cross-sections and integrated absorption cross-sections for the emission band, $^4F_{3/2} \rightarrow {}^4I_{11/2}$ at 1060 nm are high at $x = 12$ in lithium sodium glass and at $x = 24$ in lithium potassium glass. Hence, among all the glasses studied, lithium sodium glass with $x = 12$ and lithium potassium glass with $x = 24$ are more useful for laser excitation.

Acknowledgements

The author YCR expresses his thanks to the University Grants Commission for providing the financial assistance in the form of major research project. He also expresses his thanks to Prof. K. Ravindra Prasad, Head, Department of Physics, Prof. N. Prabhakara Rao, Special Officer and Dr. B. Nagaraja, Assistant Professor for their help and encouragement in the execution of the above work.

References

[1] A.D. Pearson, S.P.S. Porto, W.R. Northover, J. Appl. Phys. 73 (1993) 8066.
[2] R. Reisfeld, C.K. Jorgensen, Lasers and Excited states of Rare Earths, Springer, Berlin, 1977.
[3] M. Dejneka, B. Samson, Mater. Res. Soc. Bull. 24 (1999) 39.
[4] M.J. Weber, J. Non-Cryst. Solids 42 (1980) 189.
[5] M.J. Weber, R. Jacobs, Laser Program Annual Report-1974, Lawrence Livermore Laboratory, 1975.
[6] R.R. Jacobs, M.J. Weber, IEEE Quantum Electron QE-12 (1976) 102.
[7] B.R. Judd, Phy. Rev. 127 (1962) 750.
[8] G.S. Ofelt, J. Chem. Phys. 37 (1962) 511.
[9] K. Gatterer, G. Pucker, H.F. Fritzer, S. Arafa, J. Non-Cryst. Solids 176 (1994) 237.
[10] M.B. Saisudha, J. Ramakrishna, Phys. Rev. B. 53 (10) (1996) 6186.
[11] K. Binnemans, R. van Deun, C. Gorller-Walrand, J.L. Adam, J. Alloys, Compounds 275 (1998) 455.
[12] H. Li, L. Li, J.D. Vienna, M. Qian, Z. Wang, J.G. Darab, D.K. Peeler, J. Non-Cryst. Solids 278 (2000) 35.
[13] G.A. Kumar, A. Martinez, Elder De La Rosa, J. Lumin 99 (2002) 141.
[14] E. De La Rosa-Cruz, G.A. Kumar, L.A. Diaz-Torrs, A. Martinez, O. Barbosa-Garcia, Opt. Mater. 18 (2001) 321.
[15] H. Rawson, Inorganic Glass Forming Systems, Academic Press, London, 1967.
[16] B.C.L. Chong, S.H. Choo, S. Feller, B. Teoh, O. Mathews, E.J. Khaw, D. Fell, K.H. Chong, M. Affatigato, D. Bain, K. Hazen, K. Farooqu, J. Non-Cryst. Solids 109 (1989) 105.
[17] Y.C. Ratnakaram, R.P.S. Chakradhar, K.P. Ramesh, J.L. Rao, J. Ramakrishna, J. Phys. C: Condens. Matter 15 (2003) 6715.
[18] Y.C. Ratnakaram, Md. Abdul Altaf, R.P.S. Chakradhar, J.L. Rao, J. Ramakrishna, Phys. Stat. Sol. B 236 (1) (2003) 200.
[19] E.Y. Wong, J. Chem. Phys. 35 (1961) 544.
[20] R. Reisfeld, Struc. Bonding 22 (1975) 123.
[21] W.T. Carnall, H. Crosswhite, H.M. Crosswhite, Energy Level Structure and Transition Probabilities of Trivalent Lanthanides in LaF3, Argonne National Laboratory Report, 1977.
[22] E.W.J.L. Oomen, A.M.A. Van Dongen, J. Non-Cryst. Solids 111 (1989) 205.
[23] R. Reisfeld, C.K. Jorgensen, Excited state phenomena in vitreous materials, in K.A. Gschneidner, L.Eyring (Eds.), Hand Book on the Physics and Chemistry of Rare Earths, Vol. 9, (North-Holland, Amsterdam, 187), 1998, p. 1 (Chapter 58).
[24] H. Takebe, K. Morinaga, T. Izumitani, J. Non-Cryst. Solids 178 (1994) 58.
[25] M. Yamane, Y. Asahara, Glasses for Photonics, Cambridge University Press, Cambridge, 2000.
[26] G. Ajith Kumar, P.R. Biju, N.V. Unnikrishnan, Phys. Chem. Glasses 40 (4) (1999) 219.
[27] K.A. Gschneidner Jr., Eyring L, Hand Book on the Physics and Chemistry of Rare Earths, Vol. 25, Elsevier Publishers, North-Holland, Amsterdam, 1998.
[28] M.J. Weber, J. Non-Cryst. Solids 123 (1990) 208.